

## Supporting information for

### **High-performance lead-free quaternary antiperovskite photovoltaic candidate $\text{Ca}_6\text{N}_2\text{AsSb}$**

Yanru Guo, Xue Liu, Huaxing Wang\*, Zhigang Zang, Ru Li\*

Key Laboratory of Optoelectronic Technology & Systems (Ministry of Education), College of Optoelectronic Engineering, Chongqing University, Chongqing 400044, China.

Email: [huaxin.wang@cqu.edu.cn](mailto:huaxin.wang@cqu.edu.cn), [ru.li@cqu.edu.cn](mailto:ru.li@cqu.edu.cn)

#### **Many-body perturbation theory calculations:**

In this report, we used Quantum ESPRESSO v7.11 and YAMBO v5.1.0<sup>2</sup> to study the electronic and optical properties of quaternary antiperovskite  $\text{Ca}_6\text{N}_2\text{AsSb}$ . The whole calculation can be divided into two steps. In the first step, the structure of  $\text{Ca}_6\text{N}_2\text{AsSb}$  is relaxed until the force is less than  $10^{-4}$  Ry. YAMBO works only with Norm-conserving pseudopotentials, thus the scalar-relativistic norm-conserving pseudopotentials pseudo-dojo<sup>3</sup> is used for Quantum ESPRESSO PBE calculations, while the fully-relativistic ones are used for SOC calculations. The pseudo-dojo pseudopotentials suitable for Quantum ESPRESSO is directly download from the website with the recommended standard accuracy. For the SCF calculation, the *ecutwfc* cutoff of 100 Ry and energy convergence of  $10^{-8}$  Ry are set, the automatic K points  $5^*5^*2$  is used to sample the Brillouin zone. For the NSCF calculation, 300 bands are used and denser K points  $10^*10^*5$  are used. At the end of NSCF calculation, the database for YAMBO code is converted by the *p2y* preprocess tool. In the second step, we first converged the optics in the RPA approximation, focused on the parameters of *BndsRnXd*, *NGsBlkXd* and the k-points. To speed up the convergence with k-points, a double-grid approach is employed,<sup>4</sup> that is, a much denser k-points of  $21^*21^*10$  is re-calculated and the database is re-converted by *p2y*. After we converged the number of k-points, bands and G-vectors in optics, we started the GW calculation, for the  $G_0W_0$  calculation, we converged the *BndsRnXp*, *NGsBlkXp* and *GbndRnge*. To speed up convergence in  $G_0W_0$  calculations, the X-terminator procedure is used.<sup>5</sup> The final BSE calculation is performed on top of  $G_0W_0$  band structure, and the *BSEBands* is converged to account for the exciton effects.

Ab initio molecular dynamics (AIMD) simulations are performed by the CP2K package<sup>6</sup> in the constant temperature and constant pressure (NPT) ensemble. The temperature was controlled with a conical sampling through velocity rescaling (CSVR) thermostat at room temperature (300 K), while the pressure was controlled using an isotropic cell. The time step was set to 1.0 fs. A PBE-D3 functional was used with double-zeta basis sets (DZVP-MOLOPT) and Goedecker–Teter–Hutter pseudopotentials.<sup>7</sup> The cut-off was set to 400 Ry. The AIMD simulations were run for approximately 5 ps to ensure equilibrium.

Electron-phonon interaction calculations are carried out by open-source code EPW v5.7,<sup>8</sup> the calculation of the electron and hole mobility is divided into two steps. In the first step, the phonon calculation is performed by Quantum ESPRESSO v7.1 with Standard solid-state pseudopotentials (SSSP) efficiency (version 1.3.0), automatic K points  $5^*5^*2$  are used for the scf and phonon calculation, and *ecutwfc* cutoff of 50 Ry and energy convergence of  $10^{-8}$  Ry are set. In the second step, the Linearised Boltzmann transport

equation (BTE) is used to calculate the electron and hole mobilities, the temperature is set to 300 K and the carrier concentration is set to  $1 \times 10^{13}/\text{cm}^3$ .

For the input file preparation, the online QEtoolkit is used to help to prepare the SCF and NSCF files. High symmetry points along the 1<sup>st</sup> Brillouin zone is suggested by the online seekpath tool.<sup>9</sup> VESTA package is used to simulation the XRD patterns and display the crystal structures.<sup>10</sup> The effective mass of the electron and hole is fitted by the Python code Effmass<sup>11</sup> and the spectroscopic limited maximum efficiency (SLME) is calculated with the Python code SL3ME.<sup>12</sup> For the phonon dispersion spectrum, the Phonopy v.2.17.2<sup>13</sup> is used in conjunction with Quantum ESPRESSO v7.1, the high-symmetry path is the same to that of the electronic calculation.

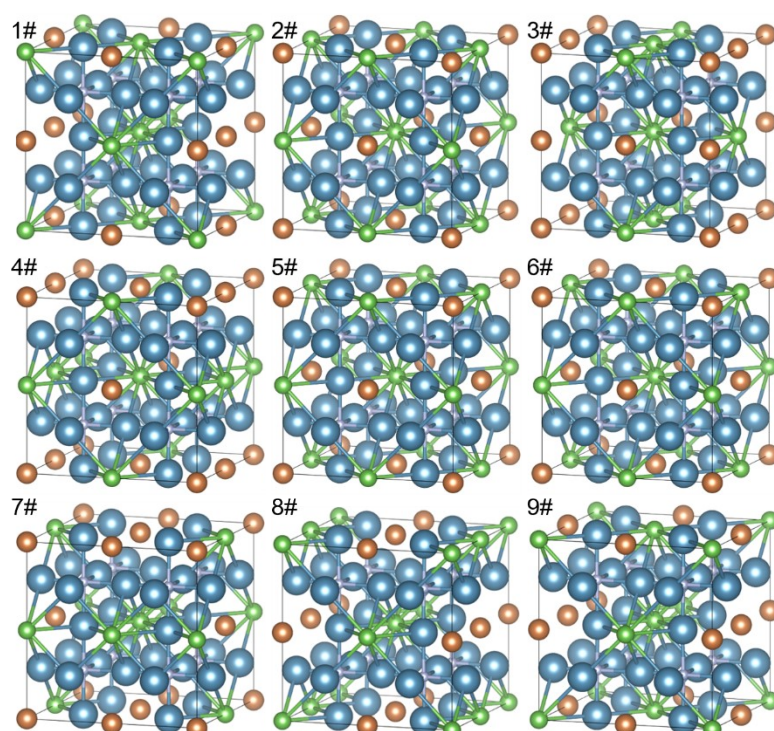


Figure S1. The 9 structures with random anion distribution.

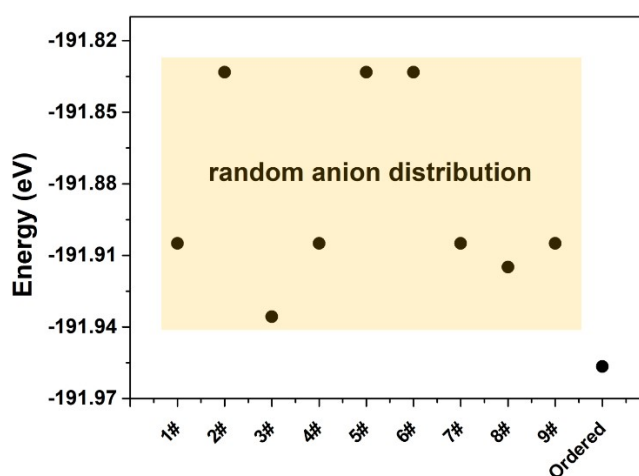


Figure S2. Total energy comparison between random anion distribution and ordered structure

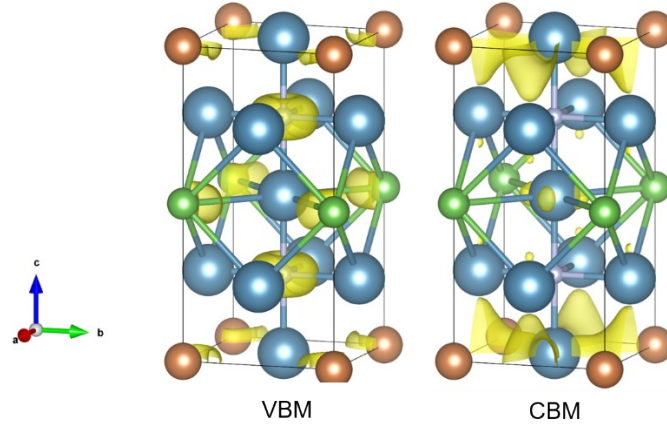


Figure S3. The charge-density isosurfaces of (a) VBM and (b) CBM states of  $\text{Ca}_6\text{N}_2\text{AsSb}$ , the isosurface level is set to 0.005.

Table S1. Effective electron and hole mass extracted from the band structure, and the electron and hole mobility calculated from electron-phonon interaction.

	$m_e$	$m_h$	$\mu_e$ (cm <sup>2</sup> /Vs)	$\mu_h$ (cm <sup>2</sup> /Vs)
Mean-field PBE	0.476	0.392	443.15 (xx/yy)	175.78 (xx/yy)
			56.54 (zz)	32.21 (zz)
Many-body GW	0.407	0.425		

- <sup>1</sup> P. Giannozzi, O. Andreussi, T. Brumme, O. Bunau, M. Buongiorno Nardelli, M. Calandra, R. Car, C. Cavazzoni, D. Ceresoli, M. Cococcioni, N. Colonna, I. Carnimeo, A. Dal Corso, S. de Gironcoli, P. Delugas, R. A. DiStasio, A. Ferretti, A. Floris, G. Fratesi, G. Fugallo, R. Gebauer, U. Gerstmann, F. Giustino, T. Gorni, J. Jia, M. Kawamura, H. Y. Ko, A. Kokalj, E. Küçükbenli, M. Lazzeri, M. Marsili, N. Marzari, F. Mauri, N. L. Nguyen, H. V. Nguyen, A. Otero-de-la-Roza, L. Paulatto, S. Poncé, D. Rocca, R. Sabatini, B. Santra, M. Schlipf, A. P. Seitsonen, A. Smogunov, I. Timrov, T. Thonhauser, P. Umari, N. Vast, X. Wu, and S. Baroni, *Journal of Physics: Condensed Matter* **29** (46), 465901 (2017).
- <sup>2</sup> D. Sangalli, A. Ferretti, H. Miranda, C. Attaccalite, I. Marri, E. Cannuccia, P. Melo, M. Marsili, F. Paleari, A. Marrazzo, G. Prandini, P. Bonfà, M. O. Atambo, F. Affinito, M. Palumbo, A. Molina-Sánchez, C. Hogan, M. Grüning, D. Varsano, and A. Marini, *Journal of Physics: Condensed Matter* **31** (32), 325902 (2019).
- <sup>3</sup> M. J. van Setten, M. Giantomassi, E. Bousquet, M. J. Verstraete, D. R. Hamann, X. Gonze, and G. M. Rignanese, *Computer Physics Communications* **226**, 39 (2018).
- <sup>4</sup> David Kammerlander, Silvana Botti, Miguel A. L. Marques, Andrea Marini, and Claudio Attaccalite, *Physical Review B* **86** (12), 125203 (2012).
- <sup>5</sup> Fabien Bruneval and Xavier Gonze, *Physical Review B* **78** (8), 085125 (2008).
- <sup>6</sup> T. D. Kuhne, M. Iannuzzi, M. Del Ben, V. V. Rybkin, P. Seewald, F. Stein, T. Laino, R. Z. Khaliullin, O. Schutt, F. Schiffmann, D. Golze, J. Wilhelm, S. Chulkov, M. H. Bani-Hashemian, V. Weber, U. Borstnik, M. Taillefumier, A. S. Jakobovits, A. Lazzaro, H. Pabst, T. Müller, R. Schade, M. Guidon, S. Andermatt, N. Holmberg, G. K. Schenter, A. Hehn, A. Bussy, F. Belleflamme, G. Tabacchi, A. Gloss, M. Lass, I. Bethune, C. J. Mundy, C. Plessl, M. Watkins,

- J. VandeVondele, M. Krack, and J. Hutter, *J Chem Phys* **152** (19), 194103 (2020).
- 7 Joost VandeVondele and Jürg Hutter, *The Journal of Chemical Physics* **127** (11), 114105 (2007).
- 8 S. Poncé, E. R. Margine, C. Verdi, and F. Giustino, *Computer Physics Communications* **209**, 116 (2016).
- 9 Yoyo Hinuma, Giovanni Pizzi, Yu Kumagai, Fumiyasu Oba, and Isao Tanaka, *Computational Materials Science* **128**, 140 (2017).
- 10 Koichi Momma and Fujio Izumi, *Journal of Applied Crystallography* **44** (6), 1272 (2011).
- 11 Lucy D Whalley, *Journal of Open Source Software* **3** (28), 797 (2018).
- 12 Liping Yu and Alex Zunger, *Physical Review Letters* **108** (6), 068701 (2012).
- 13 Atsushi Togo and Isao Tanaka, *Scripta Materialia* **108**, 1 (2015).